Fracture Mechanics of Brittle and Ductile Specimens

Berman, Brian [1], Ghosal, Sunil [2], Lovelace, David [3], Smith, Andrew[4]

Group 20 12/8/19

***Abstract*—The purpose of this lab was to determine the mode I fracture toughness of 2024 Aluminum and Acrylic test samples by characterizing the stress intensity factors of material samples with varying sample geometry. An Instron electro-mechanical test frame was used to conduct four-point bending fracture testing on test samples containing cracks that were cut into the samples by lab instructors. The maximum force during each experiment was recorded to determine the nominal stress in each sample before failure. Using knowledge of fracture mechanics and iterative numerical methods, it was then possible to determine a curve fit for each material's stress intensity factor as a function of beam thickness which resulted in a nominal value for each material's fracture toughness. The acrylic and 2024 aluminum samples had fracture toughness's of 2720 ± 191 psi$\sqrt{in}$ and 39800 ± 1140 psi$\sqrt{in}$. In the future, it will be possible to perform these experiments to quantify a material's fracture toughness to validate material selection during design phases of future projects.**

***Index Terms*—Four-Point Bending, Fracture Toughness, Plane Strain, Stress Intensity Factor.**

I. Introduction

The objective of this lab was to characterize mode I fracture toughness (K_{IC}) and stress intensity factors (K_C) for ductile and brittle materials by preforming four-point bending tests on materials with varying beam and crack geometries. A material's K_C is a measure of how sensitive a material is to cracks and is a function of thickness, while its K_{IC} value dictates how much the material will resist failure due to deformities in plane strain. Plane strain is a condition in which the thickness of the material orthogonal to the applied forces is so large that strain in that direction is considered negligible.

In this lab, an 5967 Instron electro-mechanical test frame fitted with load and support rollers was used to create the four-point bending condition and calculate the bending moment in the crack area which is a function of the total force (P) and the horizontal distance between the load and support rollers (L)(1).

$$M = \frac{PL}{2} \tag{1}$$

The advantage of using a 4-point bending condition is that the bending moment is constant in a well-defined area under the load rollers. The constant bending moment ensures that the member will fail due to the weakest portion of the beam subject to the bending moment, which is the area with the crack. The force is calculated with Instron software which uses internal load cells to determine the applied force [1].

Fracture mechanics states that in four-point bending, the K_c for a member with a crack of zero notch radius depends strictly on the geometry of the beam and the nominal stress in the beam at failure (2-3) (Fig. 1).

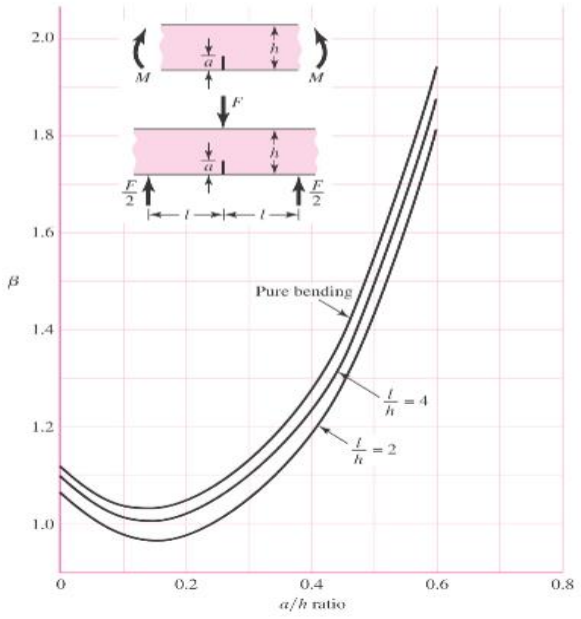

Fig. 1. β values for varying beam geometry in various states of bending [2].

$$K_c = \beta \sigma_b \sqrt{\pi a} \tag{2}$$

$$\sigma_b = \frac{6M}{th^2} \tag{3}$$

As previously stated, K_C is a function of the member's thickness. A thin member will fail in shear which is a plastic mode of failure and can be easily identified by the presence of

shear lips in the failed member. As a member's thickness is increased, more of the fracture zone will contain flat coarse grain which indicates that the member failed in tension which is a brittle mode of failure. At a certain point the fracture zone becomes completely coarse which indicates that the member is in plane strain and has a completely elastic and brittle fracture. Any increase in thickness past this point will not change the K_c value, this is considered the materials K_{IC} (Fig. 2) [2].

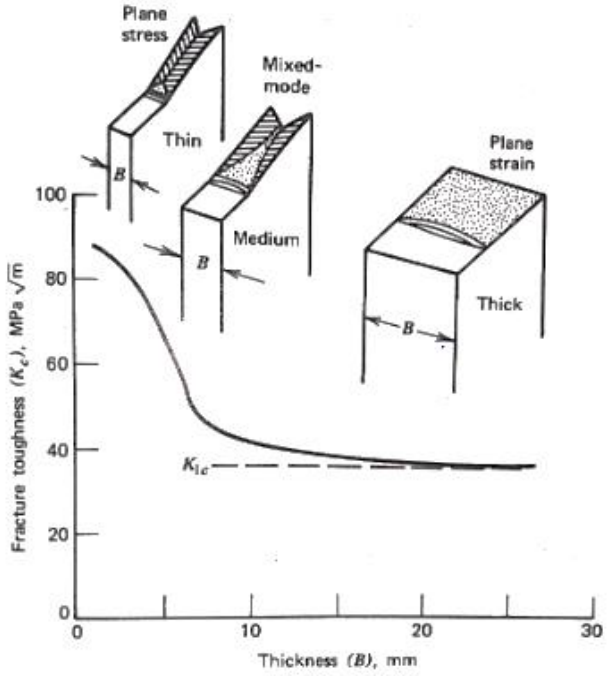

Fig. 2. Arbitrary thickness versus fracture toughness curve for an arbitrary material with images of failure modes for varying thicknesses [2].

Mathematically, K_{IC} can be determined if values for yield stress and K_C are known and if Linear Elastic Fracture Mechanics (LEFM) assumptions can be justified (4). LEFM assumptions can be made by calculating the ratio of the plastic zone radius (r_y) and the crack length (a) (5-6). Once K_{IC} is calculated it is then possible to predict if a member will exhibit plane strain based on its thickness (7).

$$K_C = K_{IC}\left(1 + \frac{1.4}{t^2}\left\{\frac{K_{IC}}{\sigma_{yp}}\right\}^4\right)^{1/2} \quad (4)$$

$$0.25 \geq \frac{r_y}{a} \quad (5)$$

$$r_y = \frac{1}{2\pi}\left(\frac{K_C}{\sigma_{yp}}\right)^2 \quad (6)$$

$$t \geq 2.5\left(\frac{K_{IC}}{\sigma_{yp}}\right)^2 \quad (7)$$

In an ideal situation, the crack and has zero notch radius. This can be created by placing a member in a fatigue loading frame until a crack begins to propogate. Unfortunatly, the lab in which the experiments were preformed did not contain such a device therefore an alternative V-notch was cut into each specimen. Theory in fracture mechanics indicates that decreasing the notch radius will decrease fracture toughness until the radius is 6.3 μm, at this point a V-notch can be considered as an ideal crack and the fracture toughness will remain constant [2]. A high powered microscope can be used to quantify crack radius in a member to ensure this criteria is met. Since the cracks are not formed naturally, there may be a large plastic zone radius at the crack tip which will yield a higher value for K_{IC} and will discredit LEFM assumptions (5). To account for this, an iteritive method can be used for cases where LEFM assumptions do not apply. The method iterates to corrrect for the large plastic zone at the crack tip until a calculated effective crack length (a') causes the iterated value of the corrected K_C (K_C') to converge to an increased calculated value that satisfies LEFM (4, 8-9).

$$K_C' = \beta'\sqrt{\pi(a' + r_y)} \quad (8)$$

$$a' = a + r_y' \quad (9)$$

II. Procedure

Materials

The materials required for this study include: Instron 5967 Universal Testing Machine (UTM) with a 30 kN load cell and a four-point bend mount, four-point bend specimens, calipers, digital microscope, micrometer, abrasive saw, razor blade, and a camera. The specimens tested by group 20 consist of two 1 x 0.5 inch acrylic bars, a 1 x 0.75 inch acrylic bar, a 1 x 0.5 inch 2024 T352 aluminum bar.

Methods

A. Preparation

The specimens were received with notches cut into them. The abrasive cutting disk that was used to cut the notches in the specimen created corners in the end of the notch. To create a simulated V-notch, each notch was scratched deeply with a razor blade. Each specimen was labelled with a permanent marker to identify it during testing.

B. Measurements

The thickness and width of each specimen was recorded with a micrometer and calipers respectively (Fig. 3). The uncertainty in the caliper measurements and micrometer measurements were half of their respective resolutions. After the notches were scored with a razor blade, the crack tip radius was measured with a digital microscope. The uncertainty in the digital microscope's measurements were calculated from two standard deviations from the mean of ten measurements resulting in a 95% confidence interval. The distance between the top two and bottom two load points on the four-point bending mount for the UTM was measured before testing. The uncertainty in the distance between the load points was measured with the mount's attached ruler.

Fig. 3. Photo of the three acrylic specimens and one 2024 aluminum specimen tested by group 20.

C. Experiment

Photos of the specimens were taken before testing. Each specimen was placed with the notch faced down between the four-point bending mount of the UTM. The lower two load points were spread farther apart than the higher two load points. With the notch faced down and the load points positioned, the face with the notch was loaded in tension. Each specimen was loaded until failure. After each catastrophic failure of the specimen, the maximum force applied to the specimen was recorded. The notched length was recorded with calipers.

D. Data Processing

The maximum recorded load, *P*, from each specimen's crack propagation test was used with the constant distance between the load rollers, *L*, to calculate the maximum moment (1). The maximum bending stress the specimen experienced was calculated from the thickness of the specimen, the height of the specimen, and the bending moment (3). The β value was calculated from a curve fit based on Figure 1 (10).

$$\beta = 1.12 - 1.39\left(\frac{a}{h}\right) + 7.3\left(\frac{a}{h}\right)^2 - 13\left(\frac{a}{h}\right)^3 + 14\left(\frac{a}{h}\right)^4 \quad (10)$$

The β value could have alternatively been estimated directly through the curve in Figure 1 from the specimen's *a/h* ratio and the *L/h* ratio. K_C was calculated for each specimen from the respective β value, bending stress, and crack length (2). The curve fit (4) of the relationship between K_C and thickness was rearranged (11).

$$(K_{\mathrm{IC}})^6 + \frac{t^2\sigma_{yp}^4}{1.4}(K_{\mathrm{IC}})^2 - \frac{t^2\sigma_{yp}^4(K_{\mathrm{C}})^2}{1.4} = 0 \quad (11)$$

To solve for K_{IC} as a root, x = $(K_{IC})^2$ was substituted into (11) to produce a cubic polynomial with three roots (12).

$$x^3 + \left(\frac{t^2\sigma_{yp}^4}{1.4}\right)x - \frac{t^2\sigma_{yp}^4(K_{\mathrm{C}})^2}{1.4} = 0 \quad (12)$$

The K_{IC} values for the 2024 aluminum and acrylic specimens were averaged. The plastic zone radius, r_y, at the crack tip at each specimen was calculated from their calculated K_C value and their yield strength (6). The yield strength for the 2024 aluminum specimen was determined from the manufacturer. The yield strength for the acrylic was determined from tensile testing done prior to experimentation. The plastic zone radius for each specimen was compared to the crack length to confirm or deny if LEFM were acceptable (5). The K_C values and the thicknesses were plotted on the y-axis and x-axis respectively. This data was grouped by material into two separate graphs. The curve fit (4) was plotted on each material's data plots keeping σ_{yp} and K_{IC} constant while varying *t*. The average K_{IC} for each material was plotted as a horizontal line with the curve fit and the data plots.

E. Uncertainty Calculations

To minimize the complexity of the uncertainty analysis, Student's *t*-distribution with a 95% confidence interval was used for a sample size of 10 and 20 for the acrylic and the 2024 aluminum respectively.

To determine the uncertainty for the acrylic and 2024 aluminum, an uncertainty for the K_C values for the sample was determined using a 95% confidence interval (13).

$$U_{K_C\ Acrylic} = t\frac{S_{KC}}{\sqrt{N}} \quad (13)$$

The *t* value for acrylic is 2.086 which corresponds to a sample size of 20, and the *t* value for 2024 aluminum is 2.201 which corresponds to a sample size of 10. The S_{KC} represents the standard deviation for the K_C values for all specimens for the acrylic and aluminum that were tested, and *N* represents the total number of specimens for the acrylic and aluminum respectively.

The nominal, maximum, and minimum K_C values can be found by adding and subtracting the K_C uncertainty from the nominal K_C for the aluminum and acrylic. The nominal values for K_{IC} were then found by solving the roots to equation (4) while using the maximum and minimum values for K_C.

$$K_{C\ max} = \mu_{K_C} + U_{K_C} \quad (14)$$

$$K_{C\ min} = \mu_{K_C} - U_{K_C} \quad (15)$$

The K_{IC} values for the corresponding maximum and minimum K_C were found by solving the real root equation (11). Once the Corresponding K_{IC} values were generated using the maximum and minimum K_C values, equation (14) was used to calculate the overall uncertainty of K_{IC}.

$$U_{K_{IC}} = K_{IC\ max} - K_{IC\ min} \quad (16)$$

III. Results

The Acrylic specimens failed under tension and exhibited a relatively smooth failure surface (Fig. 4) with a notable lack of any shear lip effect. This was unlike the aluminum specimens, which visually experienced large shear lips near the bottom edges of the material (Fig. 5).

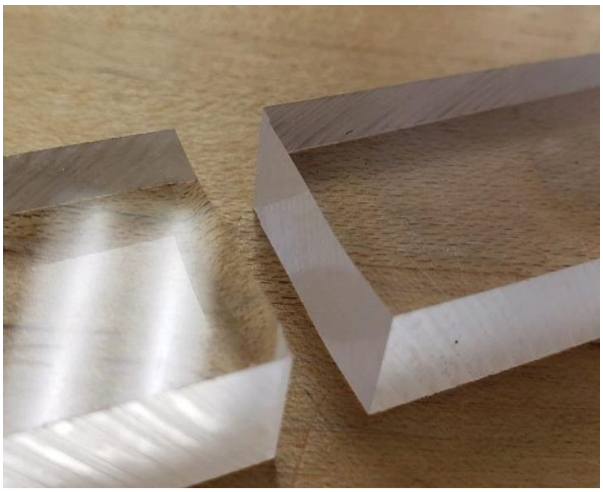

Fig. 4. The failure surface of one acrylic specimen as an example since they all failed similarly.

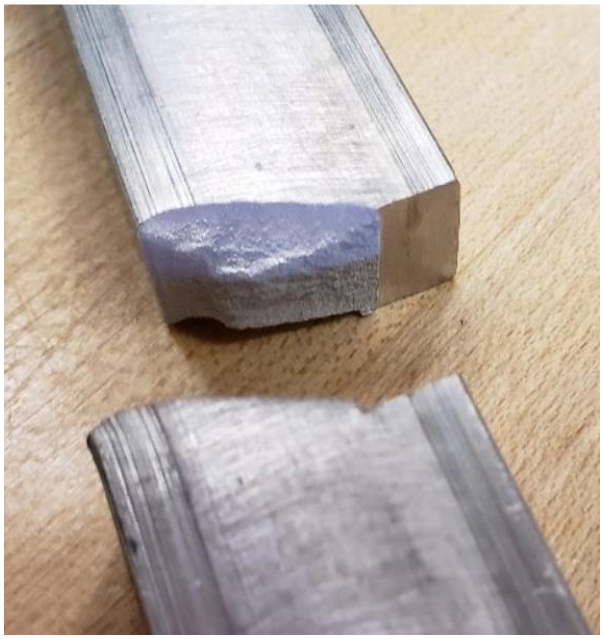

Fig. 5. The failure surface and the notched surface of the 2024 aluminum specimen.

A. *Acrylic Samples (All Groups)*

Specimen thickness for the acrylic samples ranged from 0.453 to 0.920 in. The average thickness was calculated to be 0.670 in. The acrylic minimum thickness for plane strain was found to be 0.340 in and all the acrylic specimens cleared this threshold (Fig. 9) (7). K_{IC} values ranged from 2.08 x 10^3 psi$\sqrt{in}$ to 3.67 x 10^3 psi$\sqrt{in}$ with the average value being 2.72 x 10^3 psi$\sqrt{in}$ (Table I).

TABLE I
Acrylic Sample Data

Sample Number	Thickness (in)	K_{IC} (psi$\sqrt{in}$)
#1	0.462	2.21 x 10^3
#2	0.469	2.76 x 10^3
#3	0.679	2.69 x 10^3
#9	0.92	2.85 x 10^3
#10	0.704	2.81 x 10^3
#14	0.707	2.82 x 10^3
#15	0.462	3.02 x 10^3
#16	0.943	2.71 x 10^3
#17	0.453	2.08 x 10^3
#18	0.678	2.66 x 10^3
#21	0.463	2.21 x 10^3
#22	0.952	3.47 x 10^3
#23	0.710	2.81 x 10^3
#28	0.455	2.45 x 10^3
#29	0.670	2.78 x 10^3
#30	0.953	2.55 x 10^3
#34	0.434	2.74 x 10^3
#35	0.662	2.46 x 10^3
#36	0.934	3.67 x 10^3
Average	0.670	2.72 x 10^3

Thicknesses and associated K_{IC} values for all acrylic samples

B. *Acrylic Samples (Numerical Estimation)*

The scatter plot for the K_{IC} data was graphed along with a K_{IC} curve fit using the average of the 19 K_{IC} values. The K_{IC} curve fit was calculated for thicknesses ranging from 0.2 in to 2.20 in. The K_{IC} values for 0.00 in and 0.10 in thickness were omitted because these values skewed the data (Fig 7).

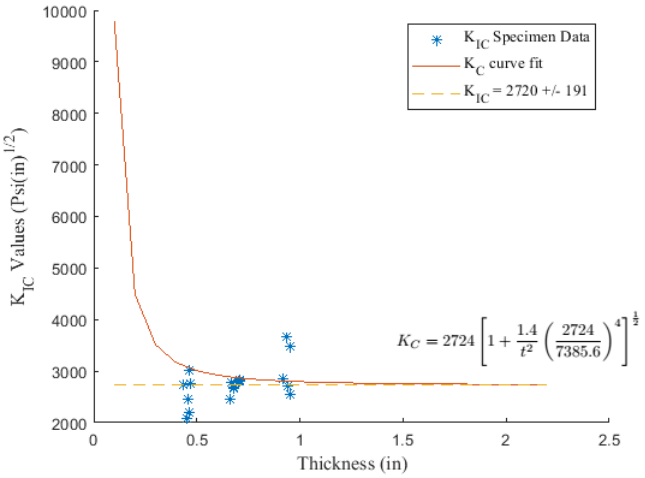

Fig. 7. Graph of the K_{IC} values specimen data over the thickness of each specimen. The K_{IC} asymptote value is denoted by the yellow dashed line.

C. *Aluminum Samples (All Groups)*

Specimen thickness for the aluminum samples ranged from 0.382 in to 0.501 in. The average thickness was calculated to be 0.429 in. The aluminum minimum thickness for plane strain was found to be 1.72 in and none of the aluminum specimens

cleared this threshold. Thus, the K_{IC} values were recalculated to account for this (8-9, 12). The specimen K_{IC} values ranged from 1.18 x 10^5 psi$\sqrt{in}$ to 8.37 x 10^5 psi$\sqrt{in}$ with the average value being 2.72 x 10^3 psi$\sqrt{in}$ (Table II).

TABLE II
Aluminum Sample Data

Sample Number	Thickness (in)	K_{IC} (psi$\sqrt{in}$)
#4	0.501	2.12 x 10^5
#11	0.502	1.24 x 10^5
#12	0.382	3.38 x 10^5
#13	0.502	1.45 x 10^5
#19	0.251	4.06 x 10^5
#20	0.500	1.29 x 10^5
#24	0.500	1.35 x 10^5
#25	0.254	3.56 x 10^5
#26	0.375	3.25 x 10^5
#27	0.500	1.18 x 10^5
#39	0.376	4.69 x 10^5
#40	0.501	8.37 x 10^5
Average	0.429	2.37 x 10^5

Thicknesses and associated K_{IC} values for all aluminum samples.

D. Aluminum Samples (Numerical Estimation)

The scatter plot for the K_{IC} data was graphed in conjunction with a K_{IC} curve fit using the average of the 12 K_{IC} values. The K_{IC} curve fit was calculated for thicknesses ranging from 0.100 in to 2.20 in (Fig 8).

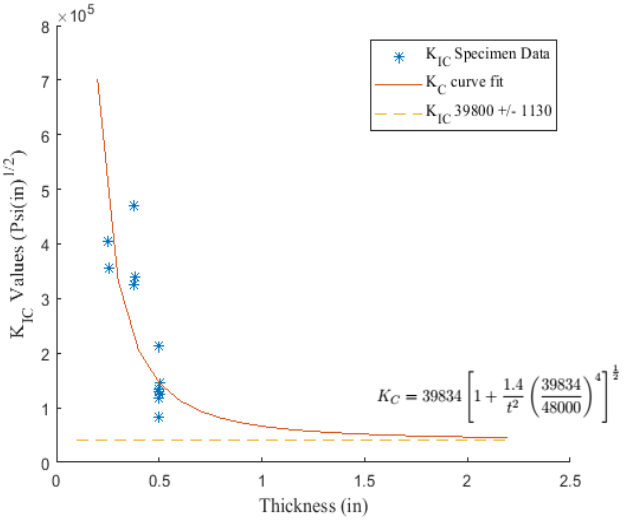

Fig. 8. Graph of the K_{IC} values specimen data over the thickness of each specimen. The K_{IC} asymptote value is denoted by the yellow dashed line.

E. Plastic Zone Calculations

Using the K_{IC} values as calculated previously, r_y was able to be found using the plane stress equation (6) for both acrylic and aluminum. These r_y values were divided by the crack length to find the ratio between the plastic zone radius and crack length $\left(\frac{r_y}{a}\right)$. These ratios were then plotted (Fig. 9)

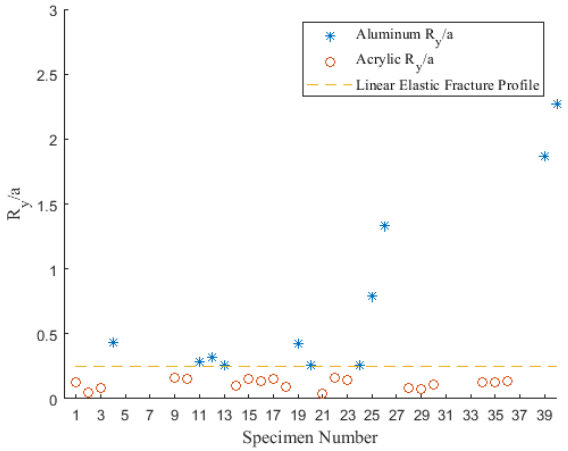

Fig. 9. The dashed yellow line denotes LEFM. Values above do not meet LEFM criteria.

IV. Discussion

The objective of this experiment was to sample twenty acrylic and ten 2024 aluminum samples to determine a mode I critical stress intensity factor. After the results were gathered, the K_{IC} values with their corresponding uncertainties were determined, and they were plotted to determine the relationship between thickness and fracture toughness (Fig. 7-8). After preforming calculations, the K_{IC} values for the acrylic and 2024 aluminum were calculated to be 2720 ± 191 psi$\sqrt{in}$ and 39800 ± 1140 psi$\sqrt{in}$ respectively. The relatively higher fracture toughness for 2024 aluminum compared to acrylic emphasizes the difference in ductility between 2024 aluminum and acrylic. With the calculated K_{IC}, the minimum thicknesses were found to be 0.34 and 1.72 inches for the acrylic and 2024 aluminum respectively. The aluminum specimens were all ½ inch or less and therefore the minimum thickness did not satisfy plane strain conditions. In the future, testing samples with thicknesses greater than the minimum thickness of 1.7 inches will yield a more accurate K_{IC}. The plane strain state reduced the uncertainty of the acrylic while the plane stress condition increased the uncertainty of the 2024 aluminum. From the physical examination of the fractured specimens after the experiment, the acrylic had a consistent clean fracture because all thicknesses satisfied plane strain conditions (Fig. 5). This implies that the plastic zones were small at the crack tip. This small plastic zone resulted in a well contained plastic zone at the crack tip which satisfies LEFM criteria. The plane stress state of the aluminum caused a plastic zone radius three times greater than plane strain conditions. From Figure 5, the 2024 aluminum experienced larger plastic zones at the crack tip and thus resulted in larger shear lips. This is intuitive because 2024 aluminum will deform plasticly before fracturing.

An important note to make is that fracture mechanics deals with cracks that have a theoretical thickness of zero. It is also shown that the K_C value decreases with decreasing crack notch radius [2]. The only way to accurately calculate a K_{IC} is to fatigue load a specimen with a stress that is about fifty percent of the yield strength. This approach requires sophisticated equipment to produce and measure the cracks. This will induce

a crack radius that is under 6μm and is equal to the grain size of the material, which when tested, will yield an accurate K_{IC} value every time. This can be done on specimens of various thicknesses to reproduce the curve fit used in this lab. With the approach that we took in this lab, the instant that the specimen experiences a load there is a large plastic zone radius and compressive residual stresses from the cutting procedure that will result in an over estimation of K_{IC}.

V. Conclusion

In conclusion, determining fracture toughness from V-notch specimens will not yield as accurate nor precise results as those collected from tests conducted with cracks created from fatigue loading, but can be used to compare the relative resistance to crack propagation between materials. It was identifiable from the data that aluminum was superior in terms of notch sensitivity since its calculated K_{IC} was roughly 15 times more than that of the acrylic. In the future, these methods and procedures can be used to evaluate trends in material fracture toughness and to determine a conservative factor of safety. To improve data precision, material samples can be made thicker to ensure the minimum thickness criteria for plane strain is met and a sharper crack can be incorporated by subjecting the test samples to fatigue loading before testing. Incorporating these improvements will greatly reduce the amount of data analysis necessary after testing and will eliminate the analysis of the plastic zone radius which decreased our data precision in every case by adding an extra degree of complexity to the numerical analysis.

Appendix

Below are the corresponding values of the maximum and minimum values of K_C using Student's t-distribution. The *A*, *B*, and *C* values represent the coefficients of equation (11). $K_{C\,max}$ and $K_{C\,min}$ are found using equations (14-15). The K_{IC} is found by solving the root to equation (11).

TABLE V
Uncertainty Analysis for K_{IC} of Acrylic

Unit	Value	Unit	Value
$K_{C\,min}\ (psi\sqrt{in})$	1.967 x 10^3	$K_{C\,max}$	3.674 x 10^3
A	1.00 x 10^0	A	1.00 x 10^0
$B\ (\frac{lb^4}{in^6})$	2.13 x 10^{15}	B	2.125 x 10^{15}
$C\ (\frac{lb^4}{in^6})$	-1.46 x 10^{22}	C	-1.944 x 10^{22}
$K_{IC\,min}\ (psi\sqrt{in})$	2.589 x 10^3	$K_{IC\,max}$	2.971 x 10^3
$U\,K_{IC}\ (psi\sqrt{in})$		1.91 x 10^2	

TABLE VI
Uncertainty Analysis for K_{IC} of 2024 Aluminum

Unit	Value	Unit	Value
$K_{C\,min}\ (psi\sqrt{in})$	7.59 x 10^4	$K_{C\,max}$	8.72 x 10^4
A	1.00 x 10^0	A	1.00 x 10^0
$B\ (\frac{lb^4}{in^6})$	9.48 x 10^{17}	B	9.48 x 10^{17}
$C\ (\frac{lb^4}{in^6})$	-7.20 x 10^{27}	C	-5.46 x 10^{27}
$K_{IC\,min}\ (psi\sqrt{in})$	3.98 x 10^4	$K_{IC\,max}$	4.21 x 10^4
$U\,K_{IC}\ (psi\sqrt{in})$		1.13 x 10^3	

References

[1] "5960 Series Universal Testing Systems." Instron. https://www.instron.us/-/media/literature-library/products/2013/02/5960-series-dual-column-tabletop-5kn--50kn.pdf?la=en-US (accessed October 14, 2019).

[2] S. Ridgeway, EML 3301C. Course Resources, Topic: "Final Group Project." Department of Mechanical & Aerospace Engineering, University of Florida, Gainesville, FL, Dec. 8, 2019